

## Using NMR to Distinguish Viscosity Effects from Nonspecific Protein Binding under Crowded Conditions

Conggang Li<sup>†</sup> and Gary J. Pielak<sup>\*,†,‡,§</sup>

Department of Chemistry, Department of Biochemistry and Biophysics, and Lineberger Comprehensive Cancer Center, University of North Carolina at Chapel Hill, Chapel Hill, North Carolina 27599

Received October 27, 2008; E-mail: gary\_pielak@unc.edu

In cells, the concentration of macromolecules can reach ~400 g/L, which makes the cell interior a heterogeneous and crowded environment.<sup>1</sup> Two consequences of crowding are high viscosity and more occupied space (excluded volume), both of which can affect protein folding, ligand binding, and protein–protein interactions.<sup>2</sup> Excluded volume effects on protein folding, stability, and function have been studied under artificial crowded conditions by using high concentrations of synthetic polymers or proteins.<sup>3–7</sup> In such studies, the crowding agent must be chemically inert with respect to the test protein. Without this property, effects attributed to excluded volume may be the result of weak interactions between the crowding molecule and the test protein or interactions of the test protein with itself. Therefore, it is important to characterize these weak interactions to distinguish crowding effects from nonspecific binding.

NMR is well suited to study weak, transient complex formation in dilute solution.<sup>8</sup> Under crowded conditions, however, the increased viscosity causes interference with these NMR-based approaches. Here, we describe an NMR method that distinguishes viscosity effects from binding and self-association in crowded solutions using a model system that contains millimolar concentrations (2–9 mg/mL) of chymotrypsin inhibitor 2 (CI2, 7.2 kDa, pI, 6.5) in 200 g/L bovine serum albumin (BSA, 66.4 kDa, pI, 4.7).

Two-dimensional heteronuclear single quantum correlation spectroscopy (HSQC) is widely used to detect weak protein interactions.<sup>8,9</sup> Crowley et al. applied this approach to show that cytochrome *c* interacts with the crowding agent poly(ethylene glycol).<sup>9</sup> For CI2, although some small chemical shift changes are detected in BSA (Supporting Information, Figure S1), this experiment does not tell us whether the changes reflect CI2–BSA binding, CI2–CI2 association, or small structural perturbations. The translational diffusion coefficient is widely used to characterize protein binding and aggregation in dilute solutions.<sup>10–12</sup> Under crowded conditions, diffusion is determined by the solution viscosity (Table S1).

Heteronuclear spin relaxation is a powerful tool for probing both the overall and the internal dynamics of proteins in dilute solution.<sup>13,14</sup> It is also utilized to characterize protein–ligand interactions, protein–protein interactions, and aggregation in dilute solution through measurement of the rotational correlation time,  $\tau_c$ .<sup>15–18</sup> In crowded solutions, however, high viscosity, binding, or self-association will also increase  $\tau_c$ , making it difficult to distinguish these instances. Kneller et al. show that the product of the longitudinal and transverse relaxation rates ( $R_1$  and  $R_2$ ) for a single population of protein is a constant that is independent of  $\tau_c$  and anisotropic motion.<sup>19</sup> A protein without conformational exchange has a maximum  $R_1R_2$  value, which is defined as the rigid

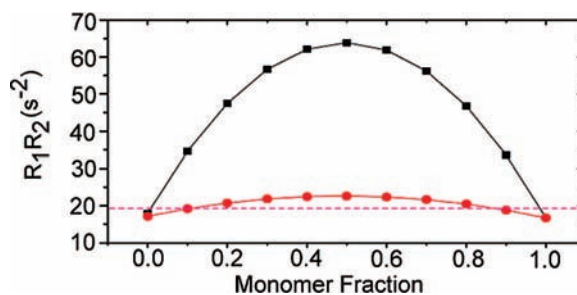


**Figure 1.** Simulated product of  $R_1R_2$  for CI2 in 200 g/L BSA, assuming only CI2•BSA heterodimers (black squares) or CI2•CI2 homodimers (red circles) as a function of the monomer fraction of CI2. The rigid limit is shown as a dashed line. The smooth curves are polynomial fits of no theoretical significance. These data are valid at 600 MHz for  $\tau_c$  values  $\geq 7$  ns.

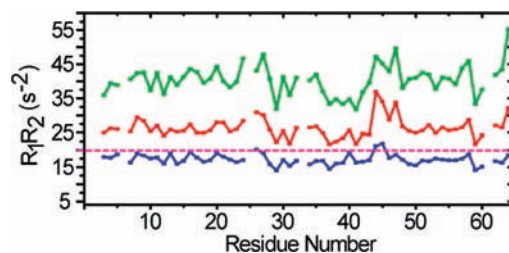


**Figure 2.** Histograms of  $R_1R_2$  values as a function of residue number for CI2 at 25 °C in 42% glycerol (blue) and 200 g/L BSA at pH 5.4 (red) and pH 6.8 (green). The rigid limit is also shown.

limit. When a protein binds another protein, simulation shows that the product of  $R_1R_2$  exceeds the rigid limit even in the absence of conformational exchange.

Simulated values of  $R_1R_2$  for CI2 in 200 g/L BSA as a function of the monomer mole fraction of CI2 are shown in Figure 1.  $R_1R_2$  for the CI2•BSA heterodimer is sensitive to the mole fraction, even when the dimer fraction is small. The maximum  $R_1R_2$  value of 65  $s^{-2}$  occurs when the solution contains half-monomer and half-heterodimer. The CI2•CI2 homodimer shows the same trend, but the amplitude is smaller. Thus, the value of  $R_1R_2$  appears to be a sensitive method that distinguishes binding from the effects of viscosity.

To test this idea,  $R_1R_2$  values for CI2 in 42% glycerol (to satisfy the criterion  $\omega\tau_c \gg 1$ ) and in 200 g/L BSA at pH 5.4 and 6.8 were measured as a function of residue number (Figure 2). The  $R_1R_2$  values for most residues in glycerol are below the rigid limit line, but a few experience conformational exchange. The  $R_1R_2$  values in BSA at pH 5.4 and 6.8 show similar patterns to those acquired in 42% glycerol, but all values are above the rigid limit line. The values at pH 6.8 are larger than those at pH 5.4, suggesting increased complex formation at the higher pH. In the simulation, the

<sup>†</sup> Department of Chemistry.

<sup>‡</sup> Department of Biochemistry and Biophysics.

<sup>§</sup> Lineberger Comprehensive Cancer Center.

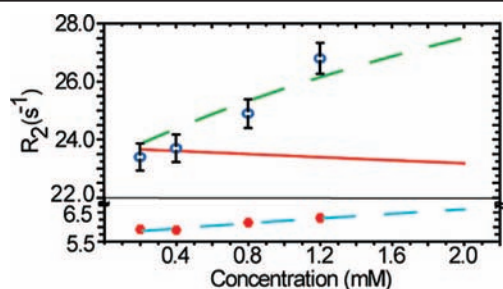


**Figure 3.** Simulated (curves) and measured (points)  $R_2$  values as a function of CI2 concentration in 200 g/L BSA (green and blue) and in buffer (cyan and orange) at pH 5.4 in sodium acetate buffer. The dashed green curve represents a CI2 homodimer ( $K_d = 15$  mM) plus a CI2•BSA heterodimer ( $K_d = 35$  mM). The red curve represents a CI2•BSA heterodimer ( $K_d = 35$  mM). The dashed cyan curve represents a CI2 homodimer in ( $K_d = 50$  mM).

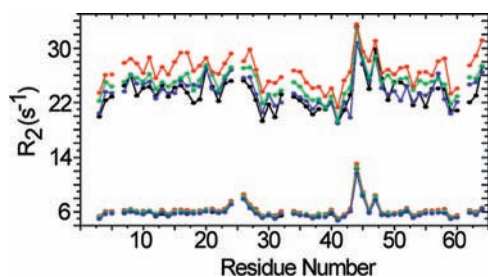


**Figure 4.** Histograms of  $R_2$  values as a function of residue number for 0.2 mM (black), 0.4 mM (blue), 0.8 mM (green), and 1.2 mM (red) CI2 at pH 5.4 in sodium acetate buffer (bottom) and in 200 g/L BSA (top). The uncertainties  $\leq 2\%$  and are not shown.

maximum value of  $R_1R_2$  is  $23 \text{ s}^{-2}$  for the CI2 monomer–dimer equilibrium. The experimentally observed average value is  $40 \text{ s}^{-2}$  at pH 6.8 and  $27 \text{ s}^{-2}$  at pH 5.4. Comparing these observations to the simulation suggest that the increased  $R_1R_2$  is mainly caused by the interaction of CI2 with BSA. The pH dependence suggests that the interaction is electrostatic.

Although formation of a CI2•BSA complex appears to be the main cause of the high  $R_1R_2$  values, there might also be a contribution from CI2 homodimer formation.<sup>20,21</sup> To investigate this possibility, we examined  $R_2$  as a function of CI2 concentration in dilute solution and in 200 g/L BSA at pH 5.4. The averaged  $R_2$  values for all residues at each of four CI2 concentrations are shown in Figure 3.  $R_2$  increases with concentration in both dilute solution and in 200 g/L BSA, as expected for protein self-association. In dilute solution the behavior is consistent with formation of a CI2 homodimer with a  $K_d$  of 50 mM. If CI2 only binds BSA, simulation shows that  $R_2$  should decrease with CI2 concentration. On the other hand, the simulated  $R_2$  values increase with concentration when CI2 forms both homodimers and a CI2•BSA heterodimer. This increase in  $R_2$  values is also observed experimentally, suggesting that CI2 forms a homodimer but that BSA has only a small effect on formation of the CI2 dimer compared to the dilute solution.

Histograms of  $R_2$  values as a function of concentration are shown in Figure 4. The  $R_2$  patterns along the sequence in buffer and 200 g/L BSA are similar, suggesting that no additional intramolecular conformational exchange occurs under crowded conditions.

We described and demonstrated here an NMR method to differentiate viscosity and binding effects under crowded conditions.

The method is based on the fact that  $R_1R_2$  is independent of viscosity and the fact that the  $R_2$  concentration dependence responds differently and sensitively to binding and self-association. The requirement that  $\omega\tau_c \gg 1$  is satisfied for most proteins in crowded conditions at high magnetic fields, so the method is general and can identify interactions of a  $^{15}\text{N}$  enriched test protein in cells or in artificial crowding environments.

Experiments aimed at quantifying the effects of excluded volume on protein chemistry must be insensitive to the unavoidable increase in viscosity brought about by crowding. At the same time such experiments must remain sensitive to nonspecific binding brought about by such large solute concentrations. The product of  $R_1$  and  $R_2$  provides a simple and reliable way to screen for truly inert crowding agents and test proteins.

In addition, binding affinities can be estimated by combining relaxation data with results from hydrodynamic calculations. CI2 self-association is enhanced slightly in 200 g/L BSA compared to a dilute solution. We cannot, however, quantify the enhancement because of the inherent uncertainties in the parameters used in the hydrodynamics calculations. It is likely that the observed CI2–BSA binding mitigates the increase in CI2 self-association expected from excluded volume effects. This conclusion shows the importance of choosing an “inert” crowding agent to study the effects of macromolecular crowding.<sup>9</sup>

**Acknowledgment.** This research was supported by a National Institutes of Health Director’s Pioneer Award (SDP10D783) and a grant from the National Science Foundation (MCB 0516547). We thank Asha Lakkavaram for help preparing CI2 samples.

**Supporting Information Available:** Sample preparation, NMR measurements, hydrodynamics calculations, and simulations. This material is available free of charge via the Internet at <http://pubs.acs.org>.

## References

- Zimmerman, S. B.; Trach, S. O. *J. Mol. Biol.* **1991**, *222*, 599–620.
- Minton, A. P.; Wilf, J. *Biochemistry* **1981**, *20*, 4821–6.
- Ai, X.; Zhou, Z.; Bai, Y.; Choy, W. Y. *J. Am. Chem. Soc.* **2006**, *128*, 3916–7.
- Charlton, L. M.; Barnes, C. O.; Li, C.; Orans, J.; Young, G. B.; Pielak, G. J. *J. Am. Chem. Soc.* **2008**, *130*, 6826–30.
- Jiang, M.; Guo, Z. *J. Am. Chem. Soc.* **2007**, *129*, 730–1.
- Totani, K.; Ihara, Y.; Matsuo, I.; Ito, Y. *J. Am. Chem. Soc.* **2008**, *130*, 2101–7.
- Zhou, H. X.; Rivas, G. N.; Minton, A. P. *Ann. Rev. Biophys.* **2008**, *37*, 375–397.
- Vaynberg, J.; Qin, J. *Trends. Biotechnol.* **2006**, *24*, 22–7.
- Crowley, P. B.; Brett, K.; Muldoon, J. *ChemBioChem* **2008**, *9*, 685–8.
- Lin, M.; Larive, C. K. *Anal. Biochem.* **1995**, *229*, 214–20.
- Ilyina, E.; Roongta, V.; Pan, H.; Woodward, C.; Mayo, K. H. *Biochemistry* **1997**, *36*, 3383–8.
- Nesmelova, I. V.; Fedotov, V. D. *Biochim. Biophys. Acta* **1998**, *1383*, 311–6.
- Korzhnev, D. M.; Kay, L. E. *Acc. Chem. Res.* **2008**, *41*, 442–51.
- Palmer, A. G., III; Massi, F. *Chem. Rev.* **2006**, *106*, 1700–19.
- Bernado, P.; Akerud, T.; Garcia de la Torre, J.; Akke, M.; Pons, M. *J. Am. Chem. Soc.* **2003**, *125*, 916–23.
- Blobel, J.; Schmid, S.; Vidal, D.; Nisius, L.; Bernado, P.; Millet, O.; Brunner, E.; Pons, M. *J. Am. Chem. Soc.* **2007**, *129*, 5946–53.
- Su, X. C.; Jergic, S.; Ozawa, K.; Burns, N. D.; Dixon, N. E.; Otting, G. *J. Biomol. NMR* **2007**, *38*, 65–72.
- Chen, K.; Bachtar, I.; Piszczek, G.; Bouamr, F.; Carter, C.; Tjandra, N. *Biochemistry* **2008**, *47*, 1928–37.
- Kneller, J. M.; Lu, M.; Bracken, C. *J. Am. Chem. Soc.* **2002**, *124*, 1852–1853.
- Snoussi, K.; Halle, B. *Biophys. J.* **2005**, *88*, 2855–66.
- Pielak, G. J.; Patel, C. N.; Winzor, D. J. *Biophys. Chem.* **2007**, *130*, 89–92.

JA808428D